Changes in the strength of the Iceland-Scotland Overflow Water in the last 200,000 years: Evidence from magnetic anisotropy analysis of core SU90-33

C. Kissel, C. Laj, B. Lehman, L. Labyrie, Viviane Bout-roumazeilles

Changes in the strength of the Iceland–Scotland Overflow Water in the last 200,000 years: Evidence from magnetic anisotropy analysis of core SU90-33

C. Kissel [a,*], C. Laj [a], B. Lehman [a], L. Labeyrie [a], V. Bout-Roumazeilles [b]

a *Centre des Faibles Radioactivités, Laboratoire mixte CNRS–CEA, Avenue de la Terrasse 91198 Gif-sur-Yvette Cedex, France*

b *Laboratoire de Sédimentologie et Géodynamique, URA 719 CNRS, Université de Lille I, 59 655 Villeneuve d'Ascq, France*

*Corresponding author. Fax: q33 1 69823568. E-mail: kissel@cfr.cnrs-gif.fr

Abstract

Results from a high resolution study of magnetic anisotropy combined with mineral magnetic analysis, clay analysis and oxygen isotopes stratigraphy are reported for core SU90-33 located (60°34'4N, 22°05'1W) at 2400 m water depth along the Iceland–Scotland overflow water (ISOW), a branch of the North Atlantic Deep Water (NADW). This core covers the last 6 climatic stages. The main magnetic mineral is low Ti-content magnetite with very slight changes in the grain size. The susceptibility record, corrected for the carbonate content, indicates down-core variations in the amount of magnetite which largely co-vary with the changes in the proportion of smectite in the clay fraction. Both parameters are climatically controlled, with lower values during glacial than during interglacial periods. The measurements of the anisotropy of magnetic susceptibility document down-core changes in the degree of anisotropy, with significantly higher values during interglacial periods than during glacial times. These changes appear to be related to differences in the degree of alignment of the magnetic particles and not to changes in grain shape, providing evidence that they arise from changes in strength of the bottom water circulation. Therefore, the strength of the contour current associated to the transport of the ISOW appears to have been significantly larger during climatic stages 5, 3 and 1 than during stages 6, 4 and 2.

Keywords: North Atlantic Deep Water; paleoclimatology; smectite; magnetite; anisotropy

1. Introduction

It is now widely recognized that the large thermohaline ocean circulation is one of the major factors driving the climate worldwide. The evaporation and cooling of the North

Atlantic surface water mass, during transportation from the equator to the northern latitudes, results in a deep convection which takes place mainly in the Greenland, Iceland and Norwegian Seas. The southward outflow of deep water back to the North Atlantic Ocean occurs both west and east of Iceland. The outflow of the Norwegian Sea Deep Water, also called the Iceland–Scot- land Overflow Water (ISOW) is thus one of the main components of the North Atlantic Deep Water (NADW) [1]. Clearly, the North Atlantic Ocean is a strategic area for the study of the circulation of this water mass of global importance [2].

Over the last 15 years, using transient tracers, many studies have contributed to a precise understanding of the present-day thermohaline circulation (see [3]). For older periods, Streeter and Shackleton [4] provided isotopic evidence suggesting that the deep water formation was largely diminished during glacial periods, a view which was also sustained by $\delta^{13}C$ studies in the Vema Channel [5] and by geochemical evidence provided by Boyle and Keigwin [6]. On the basis of oxygen isotope studies, Duplessy et al. [7, 8] have suggested that during glacial times the formation of the NADW no longer took place in the Norwegian Sea. Later, these authors also suggested that a source of cold deep water might have existed in the North Atlantic during glacial time [9]. More recently, a few geochemical and isotopic studies have been dedicated to the sub-orbital scale variability of the deep circulation in relation to the sea surface temperature changes [10, 11]. The study of sedimentological grain sizes conducted by McCave et al. [12] is the only physical approach to attempting to retrieve bottom current velocities. Changes in the sortable non carbonate silt mean obtained from cores located at the southern margin of the Rockall Bank indicate that NADW production was low during the last glacial [13]. In general (see, however [14]), most authors have agreed that production of NADW must have been depressed during glacial periods [9, 15–17].

However, despite these considerable efforts, several important characteristics, such as the response of the NADW to the huge climatic changes associated with glacial advances and retreats in the last 200,000 years, are still a subject of active research. A precise evaluation of the changes in its strength over the last climatic cycles is still lacking, and estimates vary between total suppression of the bottom water circulation [4] and a decrease during glacial periods to about 35–40% of the present day value, obtained from both $\delta^{13}C$ tracer distribution [18] and from model simulation [19, 20].

Here we present a high resolution study of the anisotropy of magnetic susceptibility of samples from Core SU90-33, obtained south of Iceland and spanning the last two climatic cycles. Although initially introduced during the early 1960s as a paleocurrent indicator [21–24], the anisotropy of the magnetic susceptibility has only seldom been used in marine studies

in recent years, principally because of the lack of commercially available equipment allowing measurements of the large number of samples necessary in these kinds of studies with the necessary sensitivity, fidelity and speed. In this study, we make systematic use of the u-channel technique in connection with a small diameter, pass-through cryogenic magnetometer to determine the direction of the natural remanent magnetization (needed to azimuthally orient the core) and of a recently developed, commercially available, anisotropy spinner magnetometer. The combination of these two modern instruments allows the necessary measurements to be carried out in reasonable time. The results show that the study of the anisotropy of magnetic susceptibility (AMS), combined with magnetic mineral and clay analysis and oxygen isotope stratigraphy in core SU90-33, allows, at least in a semi-quantitative way, reconstruction of changes in the relative strength of the contour current associated to the circulation of the North Atlantic Deep Water during the two last glacial–interglacial cycles.

2. Core location and sampling

Core SU90-33 was sampled during the PALEOCINAT cruise of the RV *Le Suroît* of IFREMER, at a water depth of 2400 m. The sampling site (longitude: 22°05'1"W; latitude: 60°34'4"N) is outside the zone affected by the massive discharges of ice-rafted material during the last glacial stage, which lies between 40°N and 55°N [25–27] (Fig. 1). The core is located on an accumulation of contourites, the Gardar Drift, built in the Icelandic Basin by the Iceland–Scotland Overflow Water (ISOW), a branch of the NADW. The local trend of the bottom topography, which basically determines the direction of the bottom flow, is about N080 at the sampling site (Fig. 1).

Directly on board a fiducial line was drawn along the plastic tube containing the sediment before cutting the core in 1.5 m segments. So, although the core was not azimuthally oriented the relative orientation of the different segments was preserved to within 5°. These segments were then split longitudinally into two halves, taking care to cut with a definite orientation with respect to the fiducial line.

Core lithology is dominated by terrigenous muddy clay and carbonate ooze with some levels of silty mud. Two types of samples were taken for the magnetic analysis along the first 11.5 m of the core. First, the working half of the core was sampled continuously using 2 X 2 X 150 cm u-channels (see e.g. [28]). Standard (2 X 2 X 2 cm) plastic cubic boxes were, in addition, used to obtain samples for the study of the anisotropy of the susceptibility. Careful attention was paid to sample these boxes with the same orientation as the u-channels. We

checked a posteriori that no distortion of the anisotropy signal was created by this sampling procedure. The core was sampled at high resolution with a cubic sample taken at 5–6 cm intervals. Only the segments of the core corresponding to climatic stages 3 and 4 were sampled at 10 cm intervals. Small amounts (ca. 0.2 g) of sediments were also sampled every 5 cm for the study of the magnetic hysteresis of the sediment.

3. Laboratory measurements and results

3.1. Oxygen isotope stratigraphy

A detailed oxygen isotope record has been obtained from planktonic foraminifera *Neogloboquadrina pachyderma sen*. (200–250 mm) and *Globigerina bulloides* (250–310 mm) from 5 shells picked for each measurement every 5–10 cm. The different laboratory techniques and the results are described elsewhere in detail [29]. The isotope measurements were performed using an automated preparation line coupled to a Finnigan MAT 251 mass spectrometer. The mean external reproducibility of powdered carbonate standards is ±0.05‰. The isotope record, shown in Fig. 2 as δ18O versus PDB using NB9 19 for calibration [30, 31], indicates that the first 11.5 m of Core SU90-33 studied here extend back in time into climatic stage 6. The sedimentation rate averages around 10 cm/kyr and does not appear to have varied conspicuously down-core.

3.2. Mineral magnetic analysis

Stepwise acquisition of the isothermal remanent magnetization (IRM) was investigated both on discrete samples up to 2.2 T using an alternating gradient field magnetometer (AGFM) and continuously on u-channels up to 0.55 T. In total, 90% of the saturation magnetization (SIRM) was acquired below 0.3 T, showing that a low coercivity mineral is the main magnetic carrier of the remanent magnetization.

Thermomagnetic analysis of bulk sediment from which the coarser fraction (>150 mm) has been removed, reveals a Curie point at 5808C, characteristic of low-Ti content magnetite (Fig. 3a). The non-reversibility of the curve upon cooling illustrates the possible formation of hematite during heating.

Down-core changes in grain size, magnetic domain state and concentration were investigated both by plotting anhysteretic remanent magnetization (ARM), imposed on u-channels using a 70 mT alternating field and a bias field of 50 mT, versus volume low-field magnetic susceptibility (χ_{lf}) [32, 33] and by analyzing ratios of hysteresis parameters. The linear trend of the data points in the ARM versus χ_{lf} plot (Fig. 3b) implies

that changes in average grain sizes are very limited, and this is also confirmed by plots of Mrs/Ms versus Hcr/Hc [34] (Fig. 3c). Within this narrow range, down-core changes in ARM/χ_{lf} indicate systematically slightly finer grains (high ARM/χ_{lf} values) during glacial isotopic stages than during interglacial stages (Fig. 3d).

In summary, the main magnetic carrier of the remanence in core SU90-33 is low Ti-content magnetite with rather uniform grain size.

3.3. Low field susceptibility and clay analysis

In core SU90-33 the carbonate fraction is always lower than 30%, except during climatic stage 5. The comparatively large detrital fraction is related to the northern location of the site. The average value of the low-field volume susceptibility (χ_{lf}) which was measured continuously on u-channels using a Bartington coil with a 3 cm resolution [28], and on the cubic specimens with a KLY 3 anisotropy spinner, is therefore rather high (>10^{-3} SI). Following Poutiers and Gonthier [35], we have combined the carbonate analysis results, the water content measurements and the magnetic susceptibility, to define the corrected susceptibility, which may be considered as a good approximation for the susceptibility of the detrital fraction of the sediment. Down-core variations in the corrected volume susceptibility (Fig. 4). Systematically document higher values during interglacial stages than during glacial stages. The analysis of the hysteresis loops determined with the AGFM shows that these changes and the rather high values observed arise from changes in the amount of ferrimagnetic low Ti-content magnetite, not from changes in the paramagnetic clay matrix. In fact, the paramagnetic contribution to the susceptibility, given by the slope of the M = f(H) at high fields ($\chi_{lf} = \chi_{para}$) never exceeds 5% of the low-field susceptibility ($\chi_{lf} = \chi_{ferri} + \chi_{para}$) (Fig. 5).

Clay analyses were conducted on the same core using X-ray diffraction analysis [36]. The details for the preparation of the samples can be found in Bout-Roumazeilles et al. [37]. The data show that well crystallized smectite and illite are the main clay minerals. A main result, shown in Fig. 4, is that the percentage of smectite in the clay mineral fraction almost perfectly covaries with the susceptibility curve and these two curves also largely mimic the oxygen isotope record.

As shown above, the susceptibility is entirely related to the magnetite content, not to the smectite. The origin of magnetites in the region where core SU90-33 has been taken is most likely the mechanical erosion of volcanic provinces such as Iceland, while smectite may

result from the chemical alteration of oceanic basalts, volcanic ashes and glasses [38]. A realistic hypothesis for the origin of this striking correlation is that the abundances of smectite and magnetite are determined by the same mechanism of transport to the site of deposition (i.e. by the bottom current). Changes in the abundance of these minerals, then, suggest that changes in the strength of the bottom current, here the ISOW, have occurred through time, a question addressed below.

3.4. Demagnetization of the NRM

To retrieve bottom current directions from this unoriented core, following other authors, we have used the average direction of the stable component of the NRM (ChRM) which, for a recording of about 200 kyr in the Brunhes chron, is best approximated by the axial dipole direction.

The direction of the characteristic remanent magnetization (ChRM) was determined from the u-channels with a small-access 2G cryogenic magnetometer. In-line AF demagnetization of the Natural Remanent Magnetization (NRM) was used throughout, with demagnetization steps at 5, 10, 20, 25, 30, 40, 50, 60 and 70 mT. Demagnetization diagrams pointing to the origin generated with 3.5 cm resolution from the u-channel measurements, accurately define the direction of the ChRM. A small viscous component is removed at 5–10 mT and the stable component of the ChRM was isolated after demagnetization in fields of the order of 20 mT (Fig. 6a). The declinations were adjusted by a constant factor so that the resulting mean declination was 0. The record of the directional characteristics (rotated declination and inclination) of the ChRM is shown in Fig. 6b. Inclination values vary between 60° and 80°; that is, around the value expected at this latitude on the basis of geocentric axial dipole field (I = 74.3°). The large inclination anomaly observed around 245 cm in isotopic stage 3 at about 37 kyr [39], where the inclination reaches 208, may correspond to the Laschamp event.

3.5. The anisotropy of magnetic susceptibility (AMS)

AMS is described by a symmetric tensor of second rank, which, in turn, may be visualized as an ellipsoid with principal axes K_1, K_2, K_3 ($K_1>K_2>K_3$) Depending on the magnetic minerals, AMS may reflect the orientation of elongated particles or crystal lattices. In the case of magnetite, as in core SU90-33, crystalline anisotropy is weak and shape anisotropy is dominant with the maximum susceptibility aligned with the long axis of the

grain. In core SU90-33, the analysis of the 'magnetic fabric' thus provides information about the preferential alignment of the elongated magnetite grains in the sediment.

AMS measurements were made with a KLY-3 Agico anisotropy spinner magnetometer. Table 1 reports the results obtained from 5 independent measurements of three different samples. The corrected degree of anisotropy, P_j, has been calculated for each sample [40]. All the samples are characterized by rather low P values varying between 1.001 and 1.034. It can be observed that, even for weakly anisotropic samples, the results are quite consistent: the direction of the principal axes is reproducible to within ±5° and the corrected degree of anisotropy to better than 0.5‰, even for values as low as 1.002. This consistency is a strong indication that the results reflect the magnetic fabric of the sediment, with negligible contribution from spurious factors, such as the noise level of the instrument. It must also be noticed that the direction of K in the sample max reference frame is different from the direction along which the sampling boxes were pushed into the sediment. The AMS is thus not related to our sampling technique.

The directions of the principal axes K_1 and K_3 obtained from all the samples of core SU90-33 are reported on stereographic projections in Fig. 7. The very large majority of the minimum axes K is close 3 to the vertical, perpendicular to the bedding plane (I_{mean} = 88°). This is typical for a sedimentary magnetic fabric, not perturbed after deposition. Within the bedding plane, the maximum axes of the AMS ellipsoid are rather well grouped, marking a magnetic lineation. This lineation, attributed in marine sediments to the presence of depositional currents [21–24], is oriented in core SU90-33 N125°±23°, after reorientation of the core in geographical coordinates. This direction is consistent within about 30° with the local topography at the location of core SU90-33.

Down-core changes in the degree of anisotropy are reported in Fig. 8. When the different climatic stages are considered separately, it can be seen that the average degree of anisotropy is larger during the interglacial than during the glacial climatic stages. Quantitatively, the average value of P_j, computed for each climatic stage using Jelinek's statistics [41] yields values of 0.3%, 0.4% and 0.3% for glacial stages 2, 4 and 6, while values of 1.3%, 1.2% and 1.8% are obtained for interglacial stages 1, 3 and 5, respectively (Table 2, Fig. 8).

4. Discussion and conclusions

Changes in the degree of anisotropy of the magnetic susceptibility of undeformed sediments may result either from changes in the distribution of shapes of individual grains or

from changes in the degree of alignment of identical grains. Only in the second case can the changes observed in core SU90-33 realistically be attributed to changes in the strength of the bottom current, here the ISOW. Although the data document that only very slight changes in grain size have occurred down-core, which would suggest that changes in grain shapes were also very limited, this point needs to be further scrutinized.

Fortunately, the data from Core SU90-33 provide self-consistent evidence that changes in the degree of alignment are the main factor affecting the degree of anisotropy. In this case one would expect changes in the K_2 intermediate axis to closely mimic changes in the K_1 axis. Indeed, because the two axis which lie in the bedding plane are by definition perpendicular to each other, any change in the degree of alignment of the K_1 axis necessarily results in a correlative change in the alignment of the K_2 axis, 90° away from it. Therefore, down-core changes in the ratio K_1/K_2 are expected to be very small (of the order of noise level) — the ratio itself being slightly over unity — and correlatively, changes in the ratio K_2/K_3 should closely mimic changes in the ratio K_1/K_3 , if indeed changes in the degree of alignment are the dominant factor affecting the degree of anisotropy. No such relations are, on the other hand, expected, when changes in the degree of anisotropy arise from changes in grain shapes. We have plotted in Fig. 9 the results obtained from core SU90-33: the ratio K_1/K_2 is on average 1.003 and displays only very small, within noise level, down-core changes (Fig. 9a) while K_1/K_3 and K_2/K_3 undergo clearly correlated changes (Fig. 9b). This is clear evidence that changes in the degree of alignment are the main factor affecting down-core changes in the degree of anisotropy in Core SU90-33. These changes may, therefore, realistically be related to changes in the strength of the ISOW.

The correlation between changes in the degree of anisotropy and the slight changes in grain size of the magnetic particles (with slightly coarser grains associated with higher degree of anisotropy) also points to the same conclusion. Indeed, while different processes can cause changes in the magnetic grain sizes, correlated changes in both variables are a good indication of bottom flow control. The results from core SU90-33 thus indicate that the strength of the contour current associated to the transport of the ISOW was significantly larger during climatic interglacial stages 5, 3 and 1 than during glacial stages 6, 4 and 2. The previous geochemical and isotopic data [9, 15–17] were interpreted as indicating a reduced production of NADW during glacial conditions. Our results suggest that the ISOW velocity was also reduced at this time.

In addition to the long-term variations in the degree of anisotropy, we notice that each transition from interglacial to glacial periods seems to be very abrupt, in particular the

transition between stages 5 and 4, while glacial to interglacial transitions, such as Terminations I and II, are much more progressive. In the same way, changes in the degree of anisotropy within stage 5 may be related to climatic substages 5a to 5e. These short-term variations in the degree of anisotropy and their possible meaning in terms of short-term variations in the strength of the ISOW need to be further scrutinized, with several samples analysed at the same level, correlated with a more detailed benthic isotopic record.

To obtain a more quantitative interpretation of the data, the analysis of modern sediments deposited in basins with well documented bottom current velocities is needed. This is not an easy task since modern sediments are usually characterized by a high water content which, when sampled, may perturb the original orientation of the particles. In the present state of knowledge, one may only tentatively speculate that changes in AMS, as small as those reported here, may be linearly related to the strength of the bottom current. With this very rough approximation, the strength of the ISOW appears to be reduced during glacial periods to about 30–35% of its value during interglacial periods. Although this figure is consistent with the estimation given by other authors on the basis of geochemical studies and modelling [5, 19, 20], we are well aware that the hypothesis of a linear relation between changes in AMS and strength of the bottom current is only a first order speculation which needs to be controlled by careful experiments in different environments.

Our results show the usefulness of combining AMS and rock magnetic characterisations with other analyses to determine relative changes in paleocurrent velocities. The study of other cores at well chosen sites in the North Atlantic and the high resolution study of climatic stages and substages transitions, now well under way in our laboratory, will tell us whether sediments can be considered as sensitive fossil bottom current meters, as suggested by Ellwood and Ledbetter [24].

Acknowledgements

We wish to thank J.C. Duplessy for discussions. J. Stoner and P. Lohmann are also thanked for their constructive reviews. This work was supported by the Atomic Energy Commission, the Centre National de la Recherche Scientifique and by the Programme National d'Etudes de la Dynamique du Climat. This is contribution CFR 1973. ***[RV]***

References

[1] W.J. Schmitz, M.S. McCartney, On the North Atlantic circulation, Rev. Geophys. 31 (1993) 29–49.

[2] W.S. Broecker, The great ocean conveyor, Oceanography 4 (1991) 79–89.
[3] R.A. Fine, Tracers, time scales and the thermohaline circulation: the lower limb in the North Atlantic Ocean, Rev. Geophys. 33 (1995) 1353–1365.
[4] S.S. Streeter, N.J. Shackleton, Paleocirculation of the Deep North Atlantic: 150,000-year record of Benthic Foraminifera and Oxygen-18, Science 203 (1979) 168–171.
[5] W.B. Curry, G.P. Lohman, Carbon isotopic changes in Benthic Foraminifera from the Western South Atlantic: reconstruction of glacial abyssal circulation patterns, Quat. Res. 18 (1982) 218–235.
[6] E.A. Boyle, L.D. Keigwin, Deep circulation of the north Atlantic over the last 200,000 years: geochemical evidence, Science 218 (1982) 784–787.
[7] J.C. Duplessy, L. Chenouard, F. Vila, Weyl's theory of glaciation supported by isotopic study of Norwegian core K 11, Science 188 (1975) 1208–1209.
[8] J.C. Duplessy, J. Moyes, C. Pujol, Deep water formation in the North Atlantic Ocean during the last ice age, Nature 286 (1980) 479–482.
[9] J.C. Duplessy, N.J. Shackleton, R.G. Fairbanks, L. Labeyrie, D. Oppo, N. Kallel, Deepwater source variations during the last climatic cycle and their impact on the global deepwater circulation, Paleoceanography 3 (3) (1988) 343–360.
[10] L.D. Keigwin, S.J. Lehman, Deep circulation change linked to Heinrich event 1 and Younger Dryas in a middepth North Atlantic core, Paleoceanography 9 (1994) 185–194.
[11] D.W. Oppo, S.J. Lehman, Suborbital timescale variability of North Atlantic Deep Water during the past 200,000 years, Paleoceanography 10 (5) (1995) 901–910.
[12] I.N. McCave, B. Manighetti, S.G. Robinson, Sortable silt and fine sediment sizercomposition slicing: parameters for palaeocurrent speed and palaeoceanography, Paleoceanography 10 (1995) 593–610.
[13] B. Manighetti, I.N. McCave, Late Glacial and Holocene palaeocurrents around Rockall Bank, NE Atlantic Ocean, Paleoceanography 10 (1995) 611–626.
[14] M. Revel, M. Cremer, F. Grousset, L. Labeyrie, Grain-size and Sr–Nd isotopes as tracer of paleo-bottom current strength, Northeast Atlantic Ocean, Mar. Geol. 131 (1996) 233–249.
[15] N.J. Shackleton, J. Imbrie, M. Hall, Oxygen and Carbon isotope record of east Pacific core V 19-30: Implications for the formation of deep water in the late Pleistocene North Atlantic, Earth Planet. Sci. Lett. 65 (1983) 233–244.
[16] D.W. Oppo, R.G. Fairbanks, Variability in the deep and intermediate water circulation of the Atlantic during the past 25,000 years: Northern hemisphere modulation of the Southern Ocean, Earth Planet. Sci. Lett. 86 (1987) 1–15.

[17] W.S. Broecker, G.H. Denton, What drives glacial cycles?, Sci. Am. 262 (1990) 49–56.
[18] W.B. Curry, G.P. Lohman, reduced advection into Atlantic Ocean deep eastern basins during, last glaciation maximum, Nature 306 (1983) 577–580.
[19] T. Fichefet, S. Hovine, J.C. Duplessy, A model study of the Atlantic thermohaline circulation during the last glacial maximum, Nature 372 (1994) 252–255.
[20] D. Seidov, M. Sarnthein, K. Stattegger, R. Prien, M. Weinelt, North Atlantic ocean circulation during the last glacial maximum and subsequent meltwater event: a numerical model, J. Geophys. Res. 101 (1996) 16305–16332.
[21] A.I. Rees, The effects of water currents on the magnetic remanence and anisotropy of susceptibility of some sediments, Geophys. J. R. Astron. Soc. 6 (1961) 235–251.
[22] A.I. Rees, The use of anisotropy of magnetic susceptibility in the estimation of sedimentary fabric, Sedimentology 4 (1965) 257–271.
[23] N.D. Hamilton, A.I. Rees, The use of magnetic fabric in paleocurrent estimation, in: S.K. Runcorn (Ed)., Paleogeophysics, Academic, Orlando, Fla., 1970, pp. 445–464.
[24] B.B. Ellwood, M.T. Ledbetter, Antarctic bottom water fluctuations in the Vema Channel: effects of velocity changes on particle alignment and size, Earth Planet. Sci. Lett. 35 (1977)
[25] W.F. Ruddiman, Late Quaternary deposition of ice-rafted sand in the sub-polar North Atlantic (lat 40°to 65°N., Geol. Soc. Am. Bull. 88 (1977) 1813–1827.
[26] G. Bond, W. Broecker, M. Klas, R. Fairbanks, R. Lotti, J. McManus, Abrupt color changes in isotope stage 5 in North Atlantic deep sea cores: Implications for rapid change of climate-driven events, in: G. Kukla, E. Went (Eds)., Start of a Glacial, NATO ASI series, vol. I3, Springer, Berlin, 1992, pp. 185–205.
[27] F. Grousset, L. Labeyrie, J.A. Sinko, M. Cremer, G. Bond, J. Duprat, E. Cortijo, S. Huon, Patterns of ice-rafted detritus in the glacial North-Atlantic, Paleoceanography 8 (1993) 175– 192.
[28] R. Weeks, C. Laj, L. Endignoux, M. Fuller, R. Manganne, A.P. Roberts, E. Blanchard, W. Goree, Improvements in long-core measuring technique: applications in paleomagnetism and paleoceanography, Geophys. J. Int. 114 (1993) 651–662.
[29] L. Labeyrie, J.C. Duplessy, J. Duprat, A. Juillet-Leclerc, J. Moyes, E. Michel, N. Kallel, N.J. Shackleton, Changes in the vertical structure of the North Atlantic Ocean between glacial and modern times, Quat. Sci. Rev. 11 (1992) 401–413.
[30] G. Hut, Stable isotope reference samples for geochemical and hydrological investigations. Consultant Group Meeting IAEA, Vienna 16–18 Sept. 1985, Report to the Director General, International Atomic Energy Agency, Vienna, 1987.

[31] T.B. Coplen, Normalization of oxygen and hydrogen isotope data, Chem. Geol. Isot. Geosci. Sect. 72 (1988) 293–297.
[32] S.K. Banerjee, J. King, J. Marvin, A rapid method for magnetic granulometry with applications to environmental studies, Geophys. Res. Lett. 8 (1981) 333–336.
[33] J.W. King, S.K. Banerjee, J. Marvin, O. Özdemir, A comparison of different magnetic methods for determining the relative grain size of magnetite in natural materials. Some results for lake sediments, Earth Planet. Sci. Lett. 59 (1982) 404–419.
[34] R. Day, M. Fuller, V.A. Schmidt, Hysteresis properties of titano-magnetite: grain-size and compositional dependance, Phys. Earth Planet. Inter. 13 (1977) 260–267.
[35] J. Poutiers, E. Gonthier, Sur la susceptibilité magnétique des sédiments, indicateur de la dispersion du matériel volcanoclastique à partir de l'Islande et des Faeroe, Bull. Inst. Géol. Bassin d'Aquitaine 23 (1978) 214–226.
[36] V. Bout-Roumazeilles, Relations entre variabilités minéralogiques et climatiques enregistrées dans les sédiments de l'Atlantique Nord depuis les 8 derniers stades glaciaires–interglaciaires, Thesis, Univ. Lille, 1995, 249 pp.
[37] V. Bout-Roumazeilles, P. Debrabant, L. Labeyrie, H. Chamley, E. Cortijo, Latitudinal control of astronomical forcing parameters on the high resolution clay mineral distribution in the 45° to 60°N range of the North Atlantic Ocean during the past 300.000 years, Paleoceanography (in press).
[38] M. Parra, P. Delmont, A. Ferragne, C. Latouche, C. Puechmaille, Origin and evolution of smectites in recent marine sediments of the NE Atlantic, Clay Miner. 20 (1985) 335– 345.
[39] E. Cortijo, L. Labeyrie, L. Vidal, M. Vautravers, M. Chapman, J.C. Duplessy, M. Elliot, M. Arnold, J.L. Turon, G. Auffret, Changes in sea surface hydrology associated with Heinrich event 4 in the North Atlantic Ocean between 40° and 60°N, Earth Planet. Sci. Lett. 146 (1997) 29–45.
[40] V. Jelinek, Characterization of the magnetic fabric of rocks, Tectonophysics 79 (1981) 63–67.
[41] V. Jelinek, Statistical processing of magnetic susceptibility measured in groups of specimens, Stud. Geophys. Geodyn.22 (1978) 50–62.
[42] T.L. Rasmussen, E. Thomsen, L. Labeyrie, T.J.E. Van Weering, Circulation changes in the Faeroe–Shetland Channel correlating with cold events during the last glacial period (58–10 ka), Geology 24 (1996) 937–940.

[43] D.G. Martinson, N.G. Pisias, J.D. Hays, J. Imbrie, T.C. Moore, N.J. Shackleton, Age dating and the orbital theory of the Ice ages: development of a high resolution 0 to 300,000-year chronostratigraphy, Quat. Res. 27 (1987) 1–29.

Figure captions

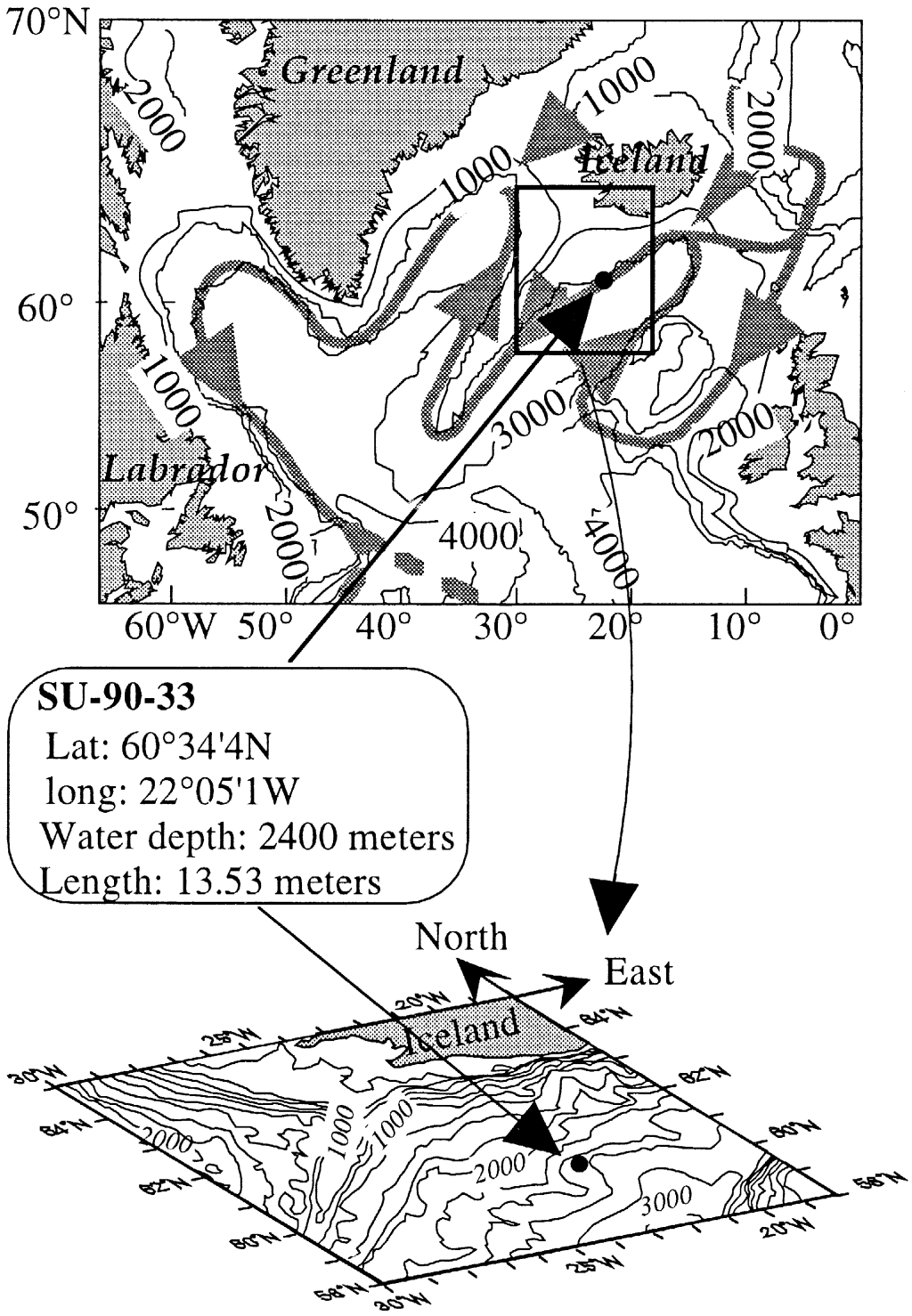

Fig. 1. Schematic map of North Atlantic (modified from [42]) showing the present-day deep water circulation and the location of core SU90-33. The bottom diagram shows more precisely the bathymetric location of the core investigated.

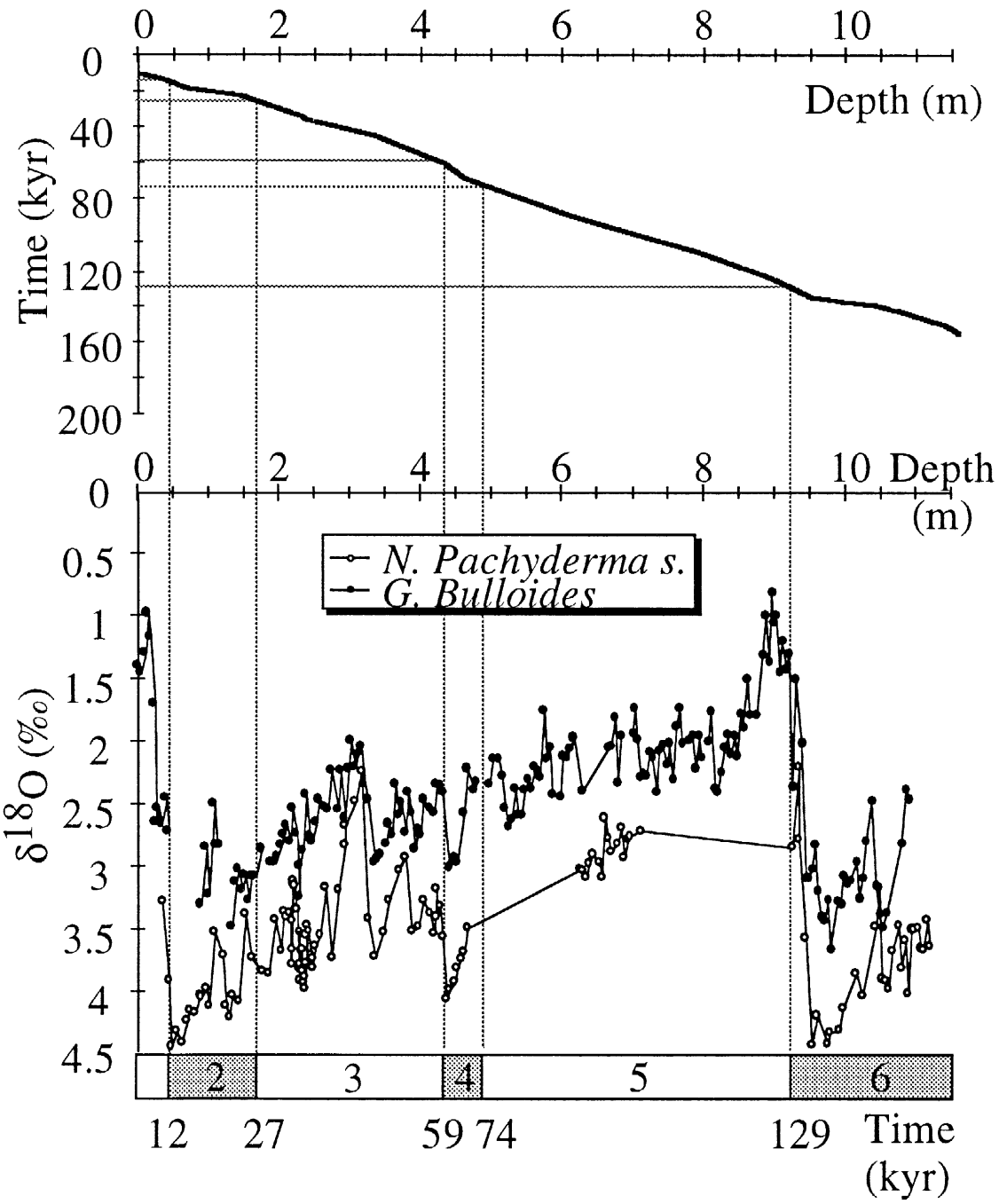

Fig. 2. The $\delta^{18}O$ record of *Globigerina Bulloides* (250–310 mm) and *Neogloboquadrina pachyderma sen*. (200–250 mm), respectively, transitional and polar planktic foraminifera in core SU90-33. The marine isotopic stages and ages, following [43], are reported for comparison. The relationship between depth and age is plotted on top of the figure.

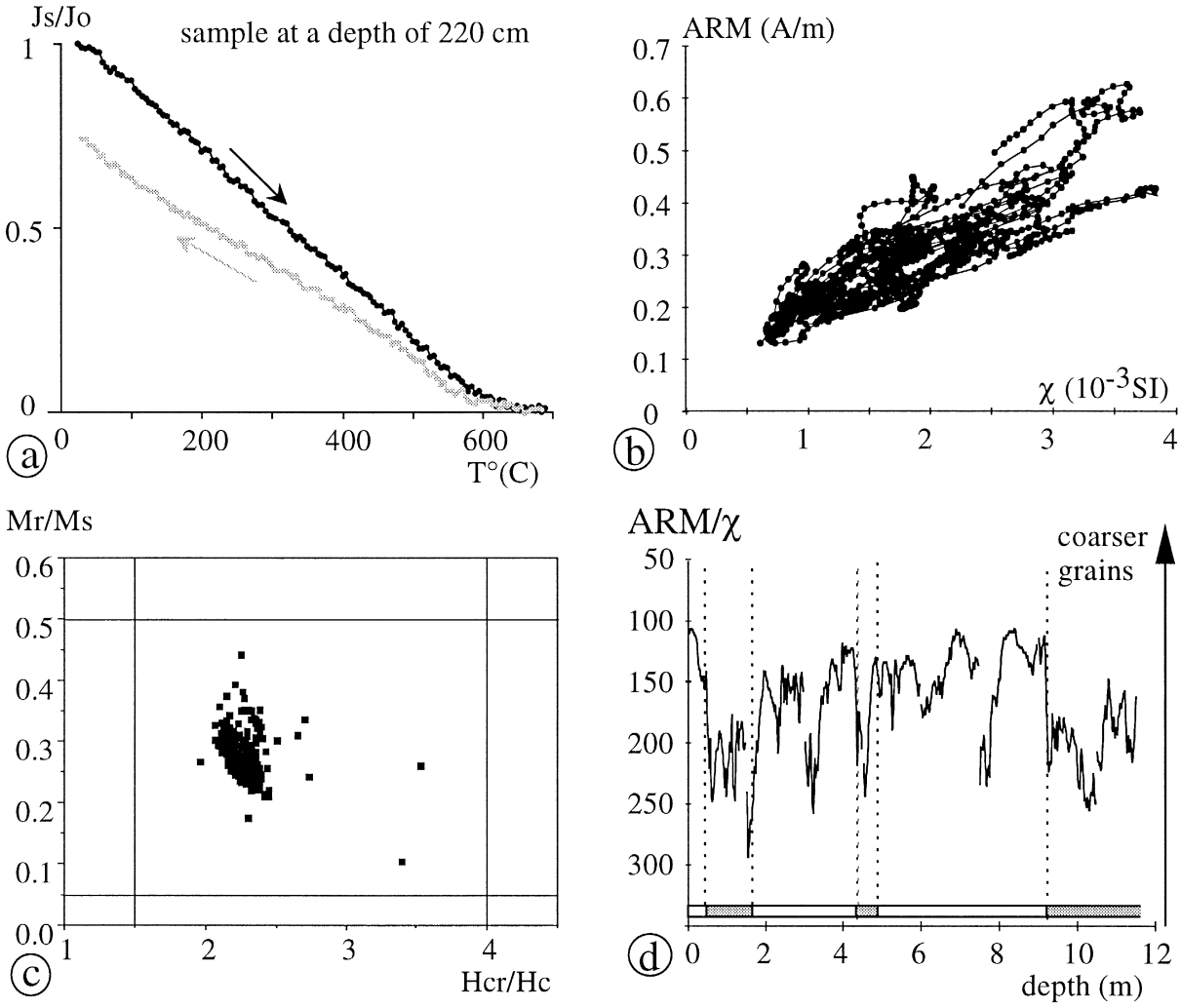

Fig. 3. Mineral magnetic analyses of core SU90-33. (a) Thermomagnetic curve obtained with an horizontal Curie balance in Argon atmosphere showing the Curie point of magnetite. (b) ARM versus χ diagram [32] indicating a uniform grain size. (c) Hysteresis ratios reported on a Day diagram [34], confirming the down-core uniformity in the average grain sizes of magnetites. (d) ARM/χ curve reported with a reverse scale versus depth (in metres).

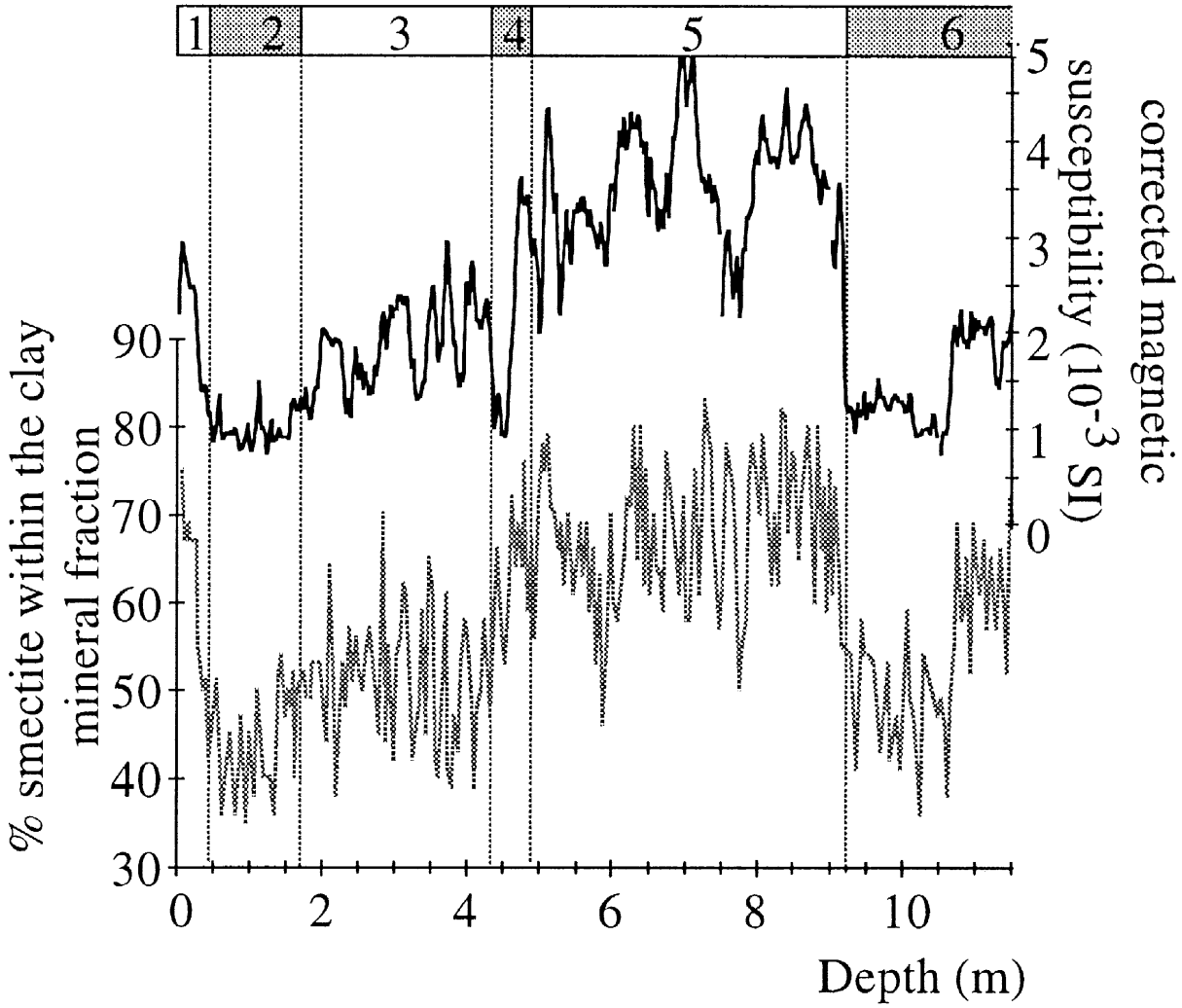

Fig. 4. Variations in the magnetic susceptibility corrected for carbonate content and water content and in the percentage of smectite within the clay fraction versus depth. Glacial periods are characterized by relatively low values of both parameters and interglacial periods by relatively high values.

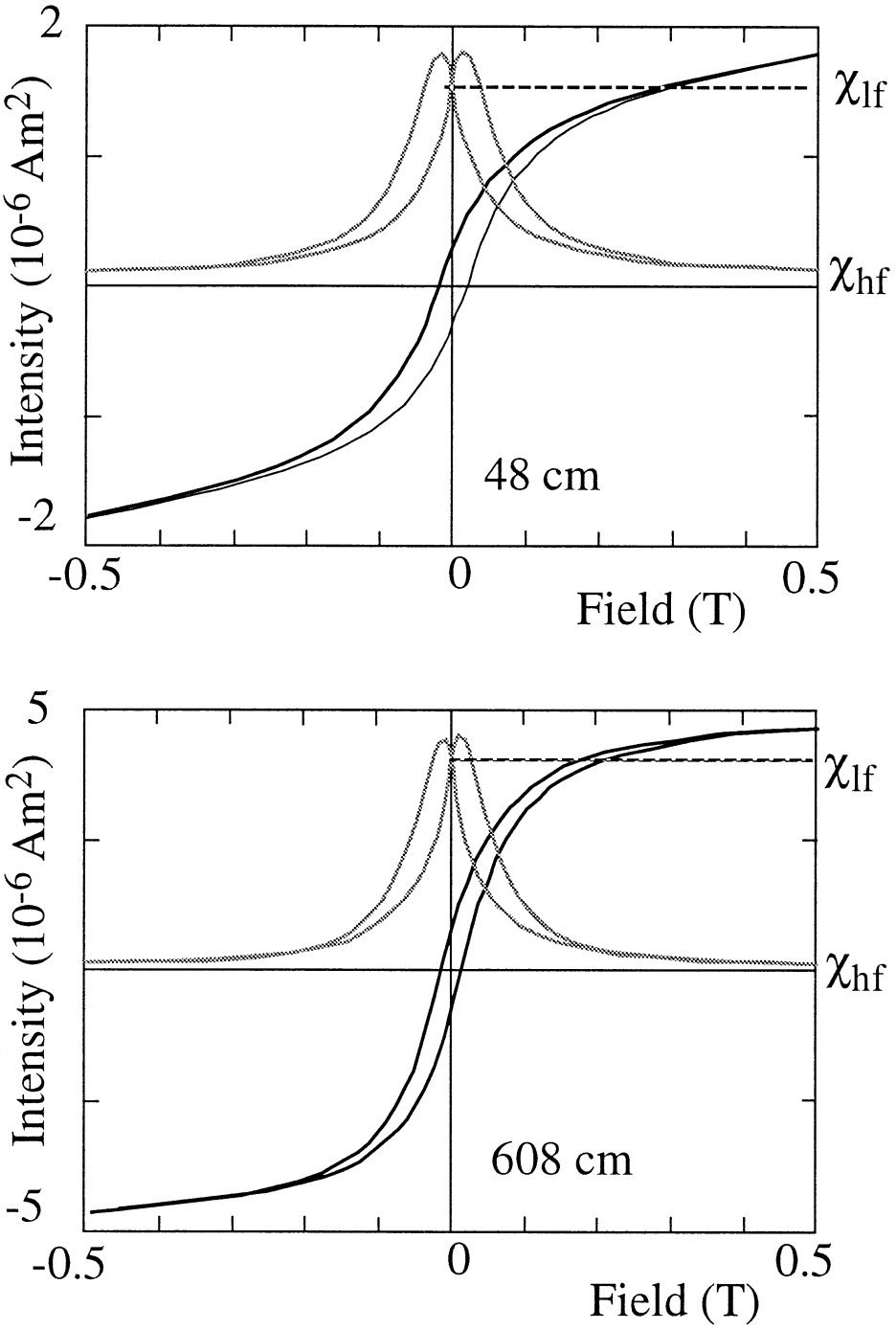

Fig. 5. Two examples of magnetic hysteresis curves obtained using an AGFM 2900. The grey curves are the derivatives of the hysteresis curves reported with black lines. They indicate that the paramagnetic fraction illustrated by the high-field susceptibility (χ_{hf}) has a very weak contribution to the low-field susceptibility (χ_{lf}).

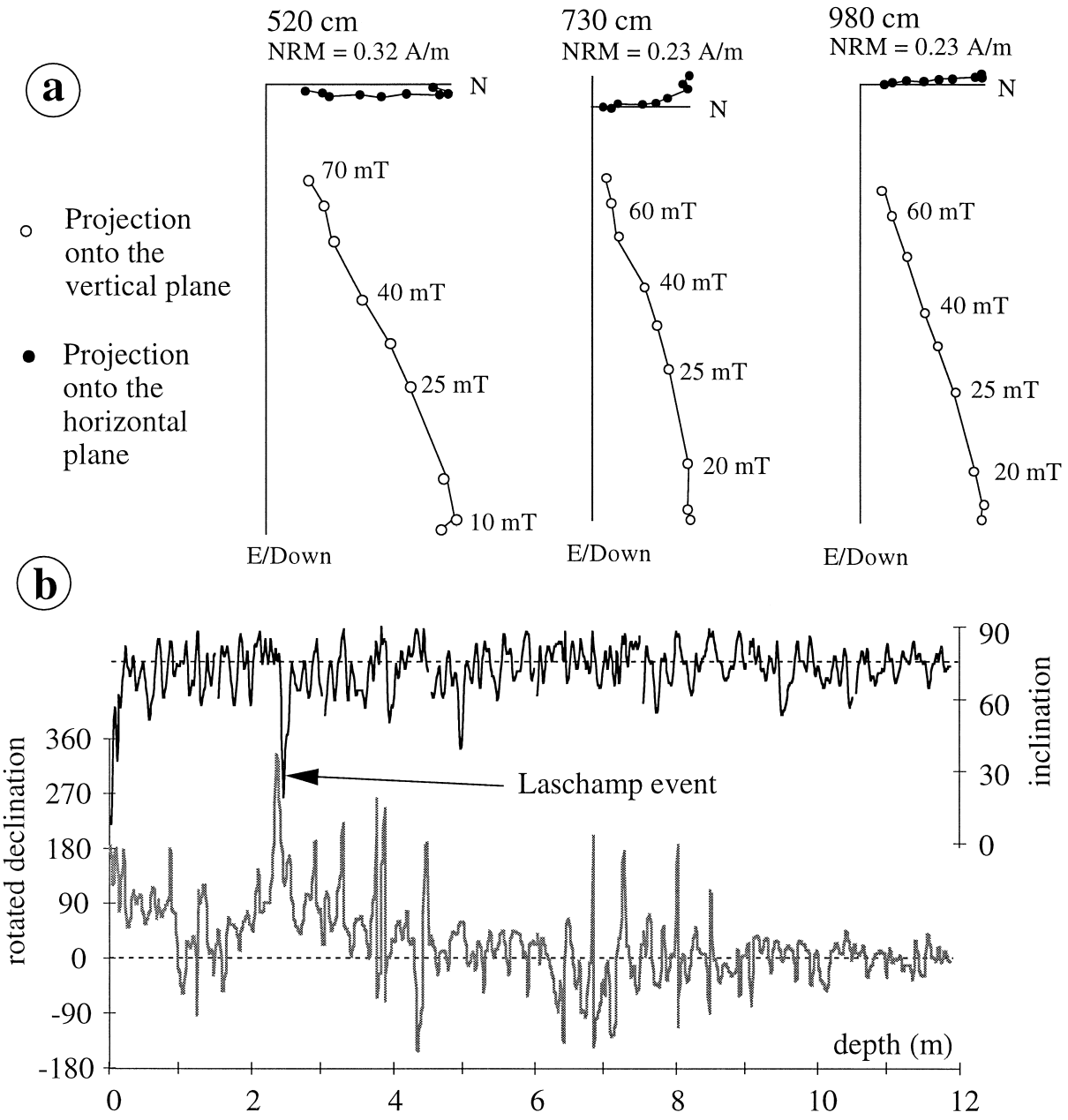

Fig. 6. (a) Demagnetisation diagrams obtained from core SU90-33. A single component of magnetisation is isolated at 10–20 mT. (b) Declination and inclination values of the characteristic remanent magnetisation versus depth. The declination is reported in geographical coordinates (see text). The dashed lines mark the present day declination and inclination values expected at the studied site on the basis of a geocentric axial dipole field (D = 0°; I = 74.3°). The Laschamp event is present both in declination and inclination at about 245 cm (i.e. about 37 kyr [39]).

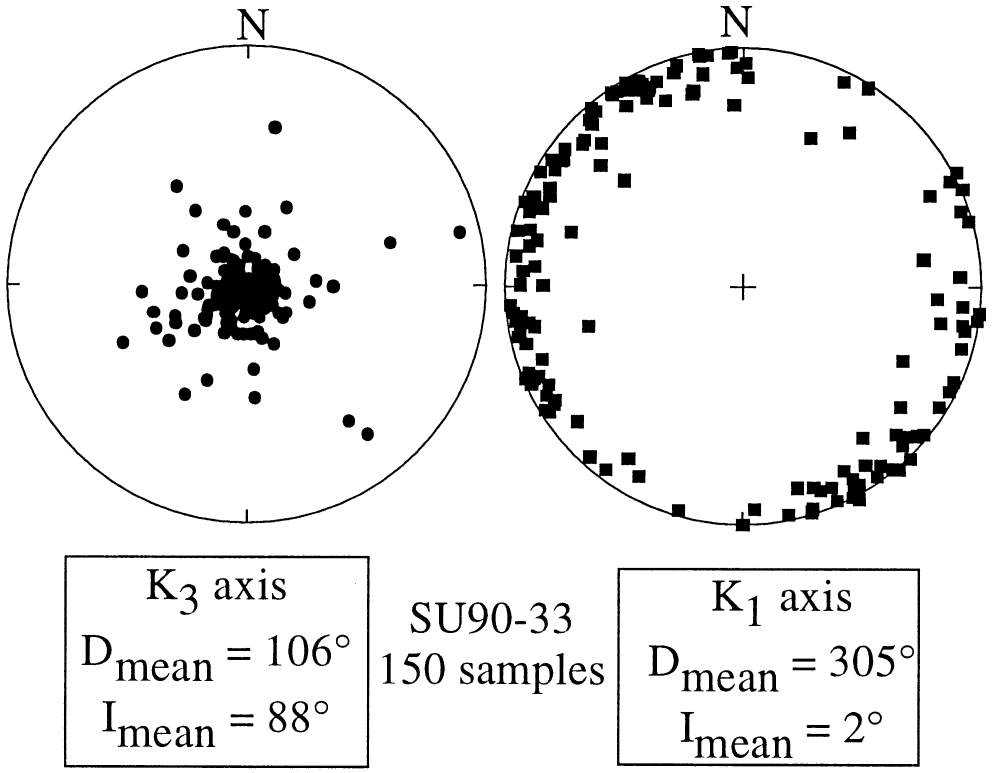

Fig. 7. Stereographic projection of the minimum (K_3) and maximum (K_1) axes of the anisotropy ellipsoids obtained from each sample. Both axes are reported with positive inclination values and declinations in geographical coordinates (see text).

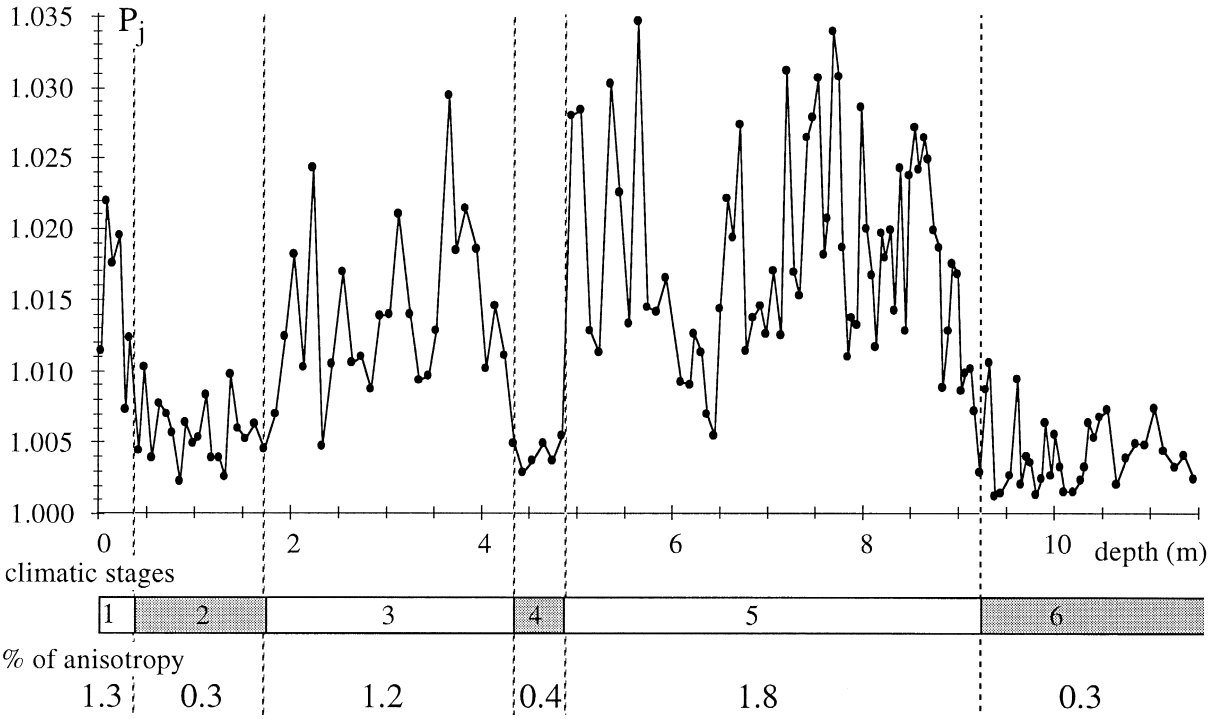

Fig. 8. Variations of the degree of anisotropy P_j versus depth (in metres). The values reported below the diagrams are the mean P_j values calculated for each climatic stage and translated in term of percentage of anisotropy $(1-P_j)/100$.

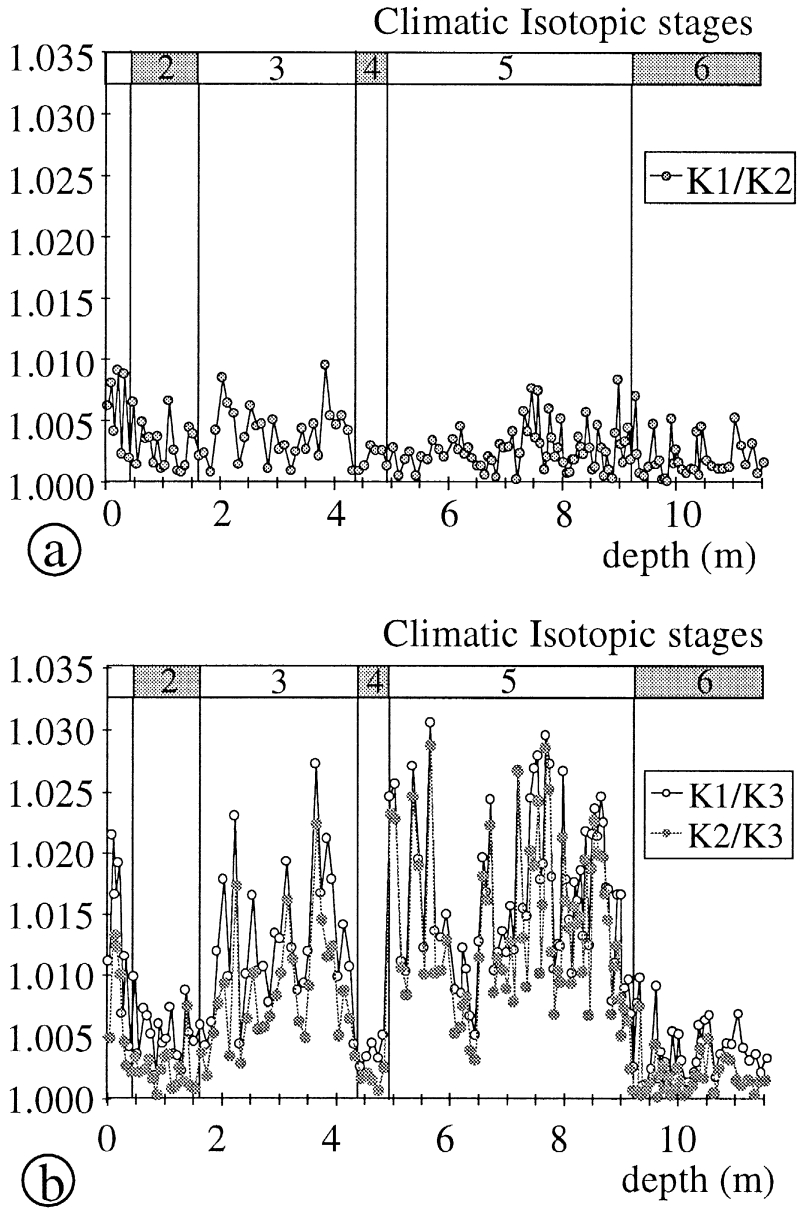

Fig. 9. Down-core changes (a) in K_1/K_2 ratio and (b) in K_1/K_3 and K_1/K_3 ratios in core SU90-33. The same scale is used for the vertical axis in both diagrams in order to show how the changes in K_1/K_2 are negligible compared to the variations in the two other ratios. The latter are thus related to variations in the degree of alignment of the magnetic particles and not to variations in the shape of the magnetite grains (see text).

Table 1

AMS results obtained from 5 successive measurements for three different samples from core SU90-33

Sample	χ (10^{-3}SI)	K_1 int.	dec.	inc.	K_2 int.	dec.	inc.	K_3 int.	dec.	inc.	P_j
444/1	1.28	1.0012	129	2	1.0003	39	15	0.9985	229	75	1.00275
444/2	1.28	1.0012	131	2	1.0003	41	15	0.9985	230	75	1.00275
444/3	1.29	1.0012	130	2	1.0002	39	15	0.9986	229	74	1.00262
444/4	1.28	1.0012	127	3	1.0002	36	16	0.9985	227	74	1.00273
444/5	1.29	1.0013	129	4	1.0002	38	13	0.9985	235	76	1.00282
84/1	8.50	1.0014	283	23	0.9994	23	17	0.9992	139	56	1.00243
84/2	8.51	1.0014	281	27	0.9994	27	27	0.9992	153	49	1.00243
84/3	8.51	1.0014	281	26	0.9994	26	25	0.9992	149	50	1.00243
84/4	8.49	1.0014	283	31	0.9995	31	28	0.9991	155	47	1.00246
84/5	8.41	1.0013	282	22	0.9995	22	18	0.9992	139	55	1.00227
1062/1	9.56	1.0009	0	1	0.9998	90	11	0.9993	262	79	1.00163
1062/2	9.58	1.0009	0	2	0.9998	91	11	0.9993	261	79	1.00163
1062/3	9.59	1.0009	0	2	0.9998	90	12	0.9993	263	78	1.00163
1062/4	9.58	1.0009	1	3	0.9999	92	13	0.9992	257	77	1.00171
1062/5	9.59	1.0009	1	2	0.9998	91	10	0.9993	261	79	1.00163

The principal axes of the anisotropy ellipsoid are defined in intensity normalized to the bulk susceptibility χ (int.), in declination (dec.) and in inclination (inc.). P_j is the factor defined by Jelinek [40] as the degree of anisotropy: $P_j = \exp\left\{\sqrt{2\left[(\ln(K_1)-\eta_m)^2+(\ln(K_2)-\eta_m)^2+(\ln(K_3)-\eta_m)^2\right]}\right\}$ with $\eta_m = [\ln(K_1)+\ln(K_2)+\ln(K_3)]/3$.

Table 2

Parameters characterizing the average AMS ellipsoid calculated for each climatic stage

Climatic stages	N	K_1			K_2			K_3			P_j	Anisotropy
		int.	dec.	inc.	int.	dec.	inc.	int.	dec.	inc.		(%)
Stage 1	6	1.006	096	1	1.001	006	−3	0.993	354	87	1.0132	1.3
Stage 2	13	1.002	090	1	1.001	000	−2	0.997	340	88	1.0030	0.3
Stage 3	28	1.005	151	−2	1.002	061	3	0.993	207	87	1.0125	1.2
Stage 4	5	1.002	162	1	1.000	074	−2	0.998	051	88	1.0040	0.4
Stage 5	66	1.006	098	−4	1.005	008	−1	0.990	087	86	1.0182	1.8
Stage 6	33	1.001	034	7	1.001	124	−2	0.998	201	83	1.0034	0.3